

# Kinetic and Thermal Modeling of Hydrothermal Carbonization Applied to Grape Marc

Marco Baratieri<sup>a</sup>, Daniele Basso<sup>b</sup>, Francesco Patuzzi<sup>a</sup>, Daniele Castello<sup>b</sup>, Luca Fiori<sup>\*b</sup>

<sup>a</sup> Free University of Bozen-Bolzano, Faculty of Science and Technology, Piazza Università 5 – 39100 Bolzano, Italy

<sup>b</sup> University of Trento, Dept. of Civil, Environmental and Mechanical Engineering, via Mesiano, 77 – 38123 Trento, Italy  
[luca.fiori@unitn.it](mailto:luca.fiori@unitn.it)

In the present investigation grape marc was processed in a HTC batch reactor at different operating conditions: 180, 220, and 250 °C and 1, 3, and 8 h residence time. The mass yield of the resulting phases (gaseous, liquid and solid) was measured. The hydrochar and gas compositions were evaluated through elemental analysis and gas-chromatography, respectively. The experimental results allowed to calibrate a kinetics model, based on a two-step reaction mechanism. The activation energy and pre-exponential factor of the various degradation reactions were determined by means of least square optimization versus the experimental data. A simplified dynamic analytic model was also built – based on lumped capacitance method – in order to simulate the thermal behavior of the system, using the actual temperature profile imposed by the reactor external heater. A resistance-capacitance network was used to describe the system, taking into account the thermo-physical properties of the systems (i.e. reactor shell, gaseous and liquid phases). This simplified tool supplemented with the calibrated kinetics model represents a first step in the characterization of the HTC process performance under different operative conditions.

## 1. Introduction

Hydrothermal carbonization (HTC) represents an emerging technology for the processing of high moisture biomass. HTC is particularly attractive in view of its relative mild operating conditions: 180 to 250 °C and a pressure in the range 10-50 bar. HTC could be intended for distributed organic waste treatment and distributed energy generation. The HTC main output is hydrochar, which can be utilized as a fuel (Castello et al., 2014) having a calorific value comparable to that of lignite, high carbon content, low degradability, high degree of homogeneity (Libra et al., 2011).

The HTC process produces also a liquid phase and a small amount of gas. The liquid phase presents several organic compounds, such as acetic acid, aldehydes and alkenes, and aromatics such as furanic and phenolic compounds (Lu et al., 2012). With respect to initial biomass charge, up to 8% of gas is produced. Experimental analyses show that the gaseous phase is mainly composed by carbon dioxide and carbon monoxide. Very small amounts of methane and hydrogen are found at high temperatures and high residence times. Considering the milder operational conditions of the process, if compared to other hydrothermal processes, such as supercritical water gasification (SCWG) (Fiori et al., 2012), HTC can represent an easy to handle treatment for organic waste with a high moisture content. For these reasons, HTC seems to be an interesting alternative to anaerobic digestion or composting.

Grape marc is extensively produced in wine-making regions and it accounts for a high moisture content (about 65 %) (Fiori and Florio, 2010) which makes it a possible candidate for HTC. Grape marc consists of grape skins, seeds and stalks which are separated before or along the wine-making process. Grape marc can result also from grappa production. Due to the large availability of this organic residue in the Trentino region (Italy), the hydrothermal process has been investigated as a promising solution to the problem of this waste disposal. Simplified engineering tools are needed for the characterization of the HTC process performance under

different operative conditions. For this purpose, in the present paper a simple kinetics model supplemented with a thermal dynamic simulation has been developed. The lumped capacitance approach - through a resistance-capacitance network - allowed the description of the thermal behavior of an experimental HTC reactor, using the thermo-physical properties of the systems and the actual operation parameters measured during some experimental runs.

## 2. Materials and methods

### 2.1 Kinetics model

For the purpose of modeling the reaction kinetics of the process, experimental data have been collected, performing the hydrothermal carbonization on grape seeds at three different temperatures (180, 220 and 250 °C) and at three residence times (1, 3 and 8 h) by means of the experimental apparatus and procedures previously described (Fiori et al., 2014, Basso et al., 2015). The substrate to water ratio ( $\text{kg}_{\text{dry substrate}}/\text{kg}_{\text{water}}$ ) was kept equal to 0.3 for all the experiments, with a biomass charge of 6.1 g and 20.4 g of deionised water, both loaded into the reactor. The mass balance of the process has been assessed by measuring the solid, the gaseous and the liquid products yields. The solid product has been characterized by elemental and calorimetric analyses, while the gaseous products have been analyzed through a portable gas chromatograph (3000 microGC, SRA Instruments).

The experimental hydrochar yields have been used for the calibration of a two-step reaction scheme, based on the mechanism proposed by Di Blasi and Lanzetta (1997). The proposed two-step mechanism assumes that the original biomass (compound A) forms an intermediate product (compound B), whose degradation gives the final product (compound C) as char. The formation of volatiles ( $V_1$  and  $V_2$ ) products is assumed to take place through reactions in parallel to those giving the compounds B and C respectively:



All the involved reactions were assumed to be of first order and the kinetic parameters were described by the usual Arrhenius equation:

$$k_i = k_{0,i} \exp\left(-\frac{E_{a,i}}{RT}\right) \quad i = 1, 2, V_1, V_2 \quad (2)$$

where  $k_{0,i}$  is the pre-exponential factor,  $E_{a,i}$  the activation energy,  $R$  the universal gas constant and  $T$  the temperature.

The calibration procedure has been carried out by means of a MatLab script. In this script, a function (receiving the applied temperature profile and the kinetics parameters as inputs) calculates for every experimental value (measured at a particular HTC temperature and residence time) the corresponding value predicted by the model.

### 2.2 Thermal model

A simplified thermal model, capable to simulate the transient behaviour of the HTC reactor has been developed. This analytical model is based on lumped capacitance method, which reduces the thermal system to a number of discrete components, assuming that the temperature difference inside each object is negligible. In the present case it is considered just one component, i.e. the HTC reactor, with its overall heat capacity and thermal resistance, subjected to the external heat flux by the electrical heater. The basic assumption is of constant temperature inside the reactor ( $T$ ). Besides the external heating system, the HTC reactor exchanges heat with the surroundings both through the upper ( $T_U$ ) and the lower ( $T_D$ ) surface.

A resistance-capacitance network has been used to describe the system, taking into account the thermo-physical properties of the liquid-gaseous water mixture, of the reactor shell and considering the thermal losses to the surroundings (Figure 1).

The energy balance reported in Eq(3) equals the variation of the internal energy of the system in time with the sum of the energy input by the external heater (i.e., the term dependent on  $T_H$ ) and the thermal losses ( $Q$ ).

$$C_0 \frac{dT}{d\tau} = \frac{T_H - T}{R_0} - Q \quad (3)$$

This first order ordinary differential equation with constant coefficients - whose main variable is the internal temperature of the reactor  $T$  - can be solved by firstly substituting the variable

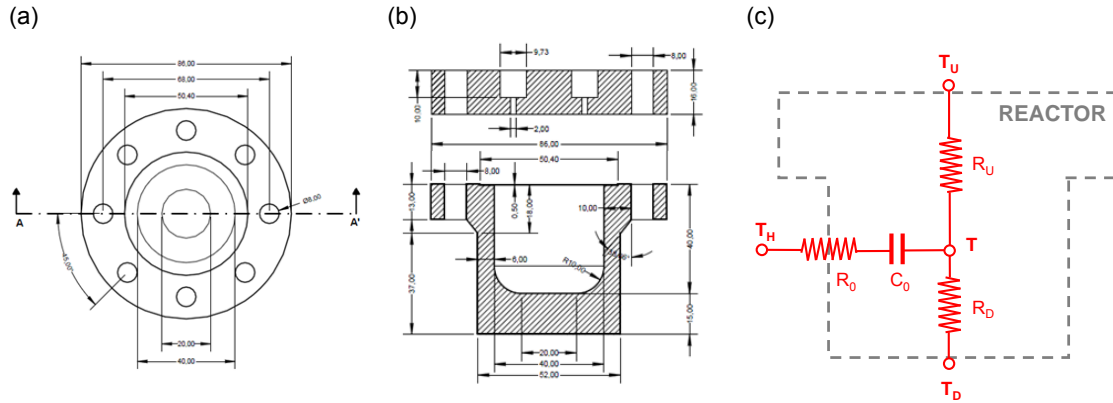


Figure 1: HRC reactor: a) top view; b) section; c) network of thermal resistances and capacities used to describe the lumped capacitance model of the HTC reactor

$$T' = T_H - T \quad (4)$$

and thus obtaining

$$\frac{dT'}{d\tau} = \frac{1}{\tau_0} (T' - QR_0) \quad (5)$$

where

$$\tau_0 = R_0 C_0 \quad (6)$$

is usually defined as the “time constant” of the system. The solution of Eq(3) is then reported in Eq(7).

$$T = (T_H - QR_0) + (T_0 - T_H + QR_0) \exp\left(-\frac{\tau}{\tau_0}\right) \quad (7)$$

The overall thermal capacity ( $C_0$ ) of the system is defined as the sum of the heat capacities of the water, i.e., considered as pure specie ( $C_W$ ), of the stainless steel shell of the reactor ( $C_{ST}$ ). Another heat storage term ( $C_{ST}$ , i.e., heat loss) is also foreseen, being the reactor positioned on a marble support.

$$C_0 = C_W + C_{ST} + \eta C_M \quad (8)$$

The different heat capacities have been computed by means of Eq(9,10,11), where  $m_i$  and  $c_i$  are the mass and the specific heat of the  $i$ -th material and specie. In the calculation of the heat capacities for saturated liquid water, the specific heat at constant volume (i.e.,  $c_{V,LIQ,W}$ ) has been assumed to be equal to the one at constant pressure (i.e.,  $c_{P,LIQ,W}$ ) while the heat capacity of saturated steam has been neglected.

$$C_W = m_W c_{L,W} \quad (c_{P,LIQ,W} \approx c_{V,LIQ,W} \approx c_{L,W}) \quad (9)$$

$$C_{ST} = m_{ST} c_{ST} \quad (10)$$

$$C_M = m_M c_M \quad (11)$$

The additional heat storage term (i.e., marble support) is multiplied by a calibration factor, assessed through the experimental tests. The specific heat at constant pressure of water has been computed as a function of the temperature using Eq(12) (Liley et al., 1997). Temperature values are expressed in Kelvin and  $c_p$  values in Joule per kmol per Kelvin. Only the liquid phase is considered.

$$c_{L,W} = 2.7637 \times 10^5 - 2.0901 \times 10^3 \cdot T + 8.1250 \cdot T^2 - 1.4416 \times 10^{-2} \cdot T^3 + 9.3701 \times 10^{-6} \cdot T^4 \quad (12)$$

The overall thermal resistance ( $R_0$ ) of the system is defined as the sum of the thermal resistance of the reactor shell (i.e., stainless steel,  $R_{ST}$ ) and the convective resistance of the water on the inner surface of the reactor ( $R_C$ ).

$$R_0 = R_{ST} + R_C \quad (13)$$

$$R_{ST} = \frac{1}{2\pi L \lambda_{ST}} \ln\left(\frac{r_{ext}}{r_{int}}\right) \quad (14)$$

$$R_C = \frac{1}{h_C (2\pi r_{int} L)} \quad (15)$$

The conductive resistance of the reactor shell (cylindrical layer) depends on the geometric parameters (see also Figure 1), as internal and external radius ( $r_{int}$ ,  $r_{ext}$ ) and height ( $L$ ) subjected to the external heating. It also depends on the thermal conductivity of stainless steel ( $\lambda_{ST}$ ). The convective resistance has been activated only for internal temperatures (i.e., water temperatures) greater than 110 °C. It depends on the internal surface area and on the convective coefficient, indirectly assessed by means of the experimental tests.

The thermal losses are defined as the sum of the losses through the upper ( $Q_U$ ) and the lower ( $Q_D$ ) surfaces depending on the relevant external temperature  $T_U$  and  $T_D$

$$Q = Q_U + Q_D = \frac{T - T_U}{R_U} + \frac{T - T_D}{R_D} \quad (16)$$

where the conductive thermal resistances - Eq(17,18) - have been computed using geometric properties - as the reactor shell thickness ( $\Delta l_U$ ,  $\Delta l_D$ , upper and lower, respectively), and the circular surface areas (upper and lower areas are considered equal) - and thermophysical ( $\lambda_{ST}$ ) properties of the reactor shell.

$$R_U = \frac{\Delta l_U}{\lambda_{ST} \pi r_{int}^2} \quad (17)$$

$$R_D = \frac{\Delta l_D}{\lambda_{ST} \pi r_{int}^2} \quad (18)$$

To test the experimental condition, also the vapour pressure ( $P$ ) has been computed through Eq(19) to be compared to the actual measured values. Eq(17) gives values in Pa and the constants can be found in (Liley et al., 1997). The whole time domain has been discretized in unit domains of 10 seconds, where the solution Eq(5) has been computed keeping constant the input parameters within them.

The temperatures and parameters introduced in the previous expressions are reported in Table 1.

$$P = \exp\left(73.649 - \frac{7258.2}{T} - 7.3037 \cdot \ln(T) + 4.1653 \times 10^{-6} \cdot T^2\right) \quad (19)$$

Table 1: Thermal, physical and geometrical parameters of the thermal model

| Parameter      | Value | Unit                               | Description   |
|----------------|-------|------------------------------------|---|
| $m_w$          | 0.026 | kg                                 | mass of water                                       |
| $m_{ST}$       | 0.842 | kg                                 | mass of stainless steel (reactor)                   |
| $m_M$          | 1.245 | kg                                 | mass of marble (support)                            |
| $c_{ST}$       | 500   | J kg <sup>-1</sup> K <sup>-1</sup> | specific heat of stainless steel (reactor)          |
| $c_M$          | 880   | J kg <sup>-1</sup> K <sup>-1</sup> | specific heat of marble (support)                   |
| $\lambda_{ST}$ | 16.3  | W m <sup>-1</sup> K <sup>-1</sup>  | thermal conductivity of stainless steel (AISI316)   |
| $h_C$          | 1225  | W m <sup>-2</sup> K <sup>-1</sup>  | thermal convection coefficient, water-reactor       |
| $r_{int}$      | 0.020 | m                                  | reactor internal radius                             |
| $r_{ext}$      | 0.026 | m                                  | reactor external radius                             |
| $L$            | 0.04  | m                                  | reactor height                                      |
| $\eta$         | 0.1   | -                                  | calibration parameter (heat loss to marble support) |

To test the model, experimental tests were performed recording temperature data in different sections of the reactor. In particular, the temperature on the upper ( $T_U$ ), lower ( $T_D$ ) and side ( $T_H$ , i.e., the heating temperature) external surfaces of the reactor have been recorded during the experimental runs.

Thus, in order to simulate the thermal behaviour of the system, the actual temperature profile has been used to represent the input by the reactor external heater, i.e. Eq(3), while the temperature on the upper and lower surfaces have been used to compute the thermal losses through the shell, i.e., Eq(14).

### 3. Results and discussion

#### 3.1 Kinetics model

Results of the kinetics model calibration are reported in Figure 2a. The values of the model parameters that give the best fit of the experimental data are:  $3.34 \cdot 10^7$ ,  $1.10 \cdot 10^{10}$ ,  $9.15 \cdot 10^6$  and  $1.55 \cdot 10^{10} \text{ s}^{-1}$  for  $k_{0,1}$ ,  $k_{0,2}$ ,  $k_{0,V1}$  and  $k_{0,2}$  respectively, and 94.5, 139.7, 93.7 and 146.2 kJ/mol for  $E_{a,1}$ ,  $E_{a,2}$ ,  $E_{a,V1}$  and  $E_{a,V2}$  respectively. As it can be observed, the model fits with satisfying accuracy the experimental data. The first reaction step results significantly faster than the second, since the activation energies in the former are smaller than those in the latter. Consequently, for low temperature ranges, the conversion yield of the compound C is very small and roughly negligible (i.e., the two-step scheme can be reduced to a single step reaction). This is clearly shown in Figure 2b, where the evolution in time of the elements considered in the reaction scheme is reported for different HTC temperature.

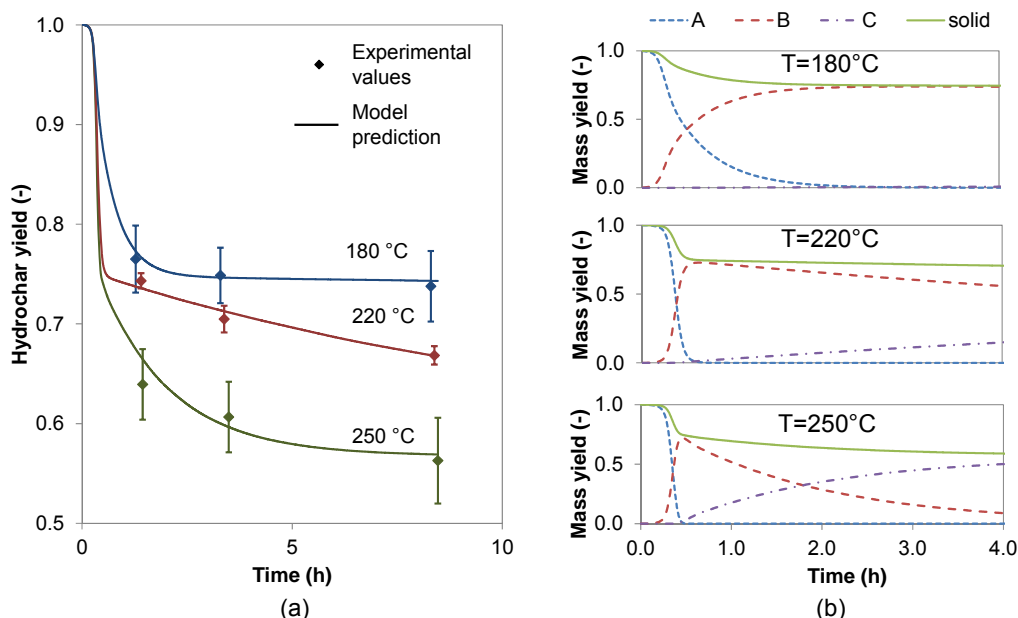


Figure 2: (a) Comparison between the experimental hydrochar yields and the predictions of the calibrated reaction model; (b) Evolution in time at different HTC temperature of the elements of the reaction scheme

#### 3.2 Thermal model

Results of the thermal simulation - applied to a run having a set point equal to 250 °C - are presented in Figure 3 where the actual measured temperature inside the reactor is compared with the modelled one. The actual heating temperature is also plotted in the figure, along with the curves of the vapour pressure, i.e., modelled and measured. The pressure values confirm that the vapour is in saturated condition until the system reaches the setup temperature. After that, the generation of gas - due to the HTC reactions - occurs inside the water mixture and causes an increase of the pressure with respect to the predicted values (e.g., increase of 2.8 bar, at 2,500 s).

The thermal behaviour of the system can be roughly represented by three different stages. A first stage of heating (until 100-110 °C), a second stage (until reaching the set point) and a plateau. The changing in the slope of the curve between the first and the second stage has been modelled introducing a convective resistance  $R_c$ .

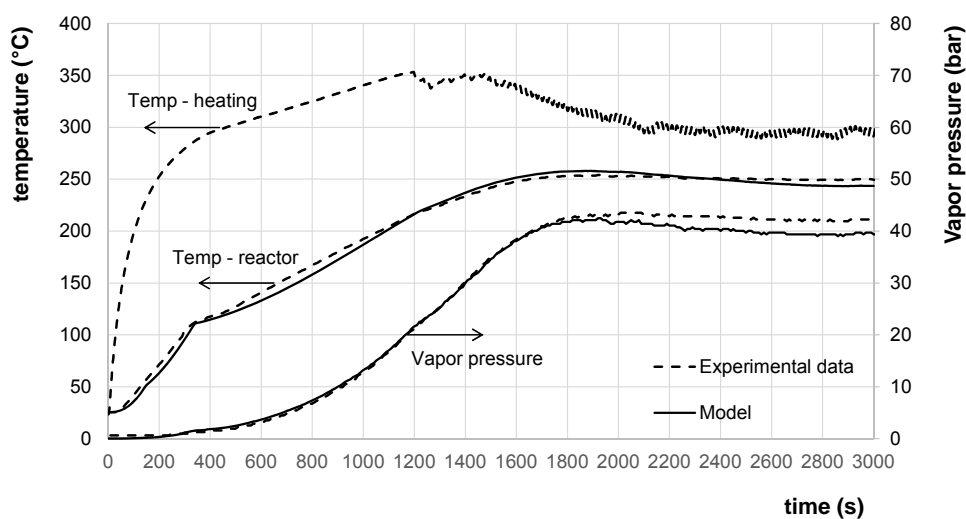


Figure 3: Thermal model: comparison between measured (dashed lines) and model (continuous lines) values of temperature and vapour pressure.

#### 4. Conclusions

A thermal dynamic model supplemented with a calibrated kinetics model has been developed in this paper. The lumped capacitance approach has been proven to be capable to describe satisfactorily the thermal behavior of an experimental HTC reactor, using the thermo-physical properties of the systems and the actual operational parameters measured during some experimental runs.

This simplified engineering tool represents a first step in the characterization of the HTC process performance under different operative conditions. Further studies are under development in order to introduce the solid and gaseous phases within the thermal model and also to couple the thermal and kinetics routines into a single model.

#### References

- Basso D., Weiss-Hortala E., Patuzzi F., Castello D., Baratieri M., Fiori L., 2015, Hydrothermal carbonization of off-specification compost: A byproduct of the organic municipal solid waste treatment, *Biores. Technol.*, 182, 217–224
- Castello D., Kruse A., Fiori L., 2014, Supercritical water gasification of hydrochar, *Chem. Eng. Res. Design*, 92 1864-1875.
- Di Blasi C., Lanzetta M., 1997, Intrinsic kinetics of isothermal xylan degradation in inert atmosphere, *J. Anal. Appl. Pyrolysis*, 40-41, 287-303
- Fiori L., Florio L., 2010, Gasification and Combustion of Grape Marc: Comparison Among Different Scenarios. *Waste and Biomass Valorization*, 1, 191–200.
- Fiori L., Valbusa M., Castello D., 2012, Supercritical water gasification of biomass for H<sub>2</sub> production: Process design, *Biores. Technol.*, 121, 139-147.
- Fiori L., Basso D., Castello D., Baratieri M., 2014, Hydrothermal Carbonization of Biomass: Design of a Batch Reactor and Preliminary Experimental Results, *Chem. Eng. Trans.*, 37, 55-60.
- Libra J.A., Ro K.S., Kammann C., Funke A., Berge N.D., Neubauer Y., Titirici M.-M., Fühner C., Bens O., Kern J., Emmerich K.H., 2011, Hydrothermal carbonization of biomass residuals: a comparative review of the chemistry, processes and applications of wet and dry pyrolysis, *Biofuels*, 2, 89-124.
- Liley P.E, Thomson G.H., Friend D.G., Daubert T.E., Buck E., 1997. Physical and Chemical Data, Section 2, in "Perry's Chemical Engineers' Handbook," 7th ed., McGraw-Hill, New York, USA.
- Lu X., Jordan B., Berge N.D., 2012, Thermal conversion of municipal solid waste via hydrothermal carbonization: comparison of carbonization products to products from current waste management techniques, *Waste Management*, 32(7), 1353–1365.